Curcumin in VIP-Targeted Sterically Stabilized Phospholipid Nanomicelles: A Novel Therapeutic Approach for Breast Cancer and Breast Cancer Stem Cells

Ece Gülçür[1, †] , Mentor Thaqi [2, †] , Fatima Khaja[1], Antonina Kuzmis[1], Hayat Önyüksel [1,2,*]

[1] *Department of Biopharmaceutical Sciences, University of Illinois at Chicago, Chicago/IL 60612, USA*

[2] *Department of Bioengineering, University of Illinois at Chicago, Chicago/IL 60607, USA*

[†] *These authors contributed equally to this work.*

* *Corresponding author.*

Department of Biopharmaceutical Sciences (M/C 865) College of Pharmacy,

University of Illinois at Chicago, 833 South Wood St.,

Chicago, Illinois 60612-7231, USA.

Tel.: +1 312 996 2097; fax: +1 312 996 0098.

E-mail address: hayat@uic.edu

Keywords:

Curcumin, sterically stabilized phospholipid micelles, nanoparticles, breast cancer stem cells, targeted drug delivery, vasoactive intestinal peptide.

Abstract

Breast cancer is a leading cause of cancer deaths among women in the US, with 40% chance of relapse after treatment. Recent studies outline the role of cancer stem cells (CSCs) in tumor initiation, propagation and regeneration of cancer. Moreover it has been established that breast CSCs reside in a quiescent state that makes them more resistant to conventional cancer therapies than bulk cancer cells resulting in tumor relapse. In this study we establish that CSCs are associated with the overexpression of vasoactive intestinal peptide (VIP) receptors which can be used to actively target these cells. We investigated the potential of using a novel curcumin nanomedicine (C-SSM) surface conjugated with VIP to target and hinder breast cancer with CSCs.

Here we formulated, characterized and evaluated the feasibility of C-SSM nanomedicine in-vitro. We investigated the cytotoxicity of C-SSM on breast cancer cells and CSCs by tumorsphere formation assay. Our results suggest that curcumin can be encapsulated in SSM up to 200 µg/ml with 1mM lipid concentration. C-SSM nanomedicine is easy to prepare, and maintains its original physicochemical properties after lyophilization, with an IC_{50} that is significantly improved from that of free curcumin (14.2 ± 1.2 µM vs. 26.1 ± 3.0 µM). Furthermore, C-SSM-VIP resulted in upto 20% inhibition of tumorsphere formation at a dose of 5 µM. To this end, our findings demonstrate the feasibility of employing our actively targeted nanomedicine as a potential therapy for CSCs enriched breast cancer.

1. Introduction

Breast cancer is the most commonly occurring cancer in females, after non-melanoma skin cancer, and the leading cause of cancer death among women in the US. Although existing chemotherapies and radiotherapies are initially effective in controlling breast tumor growth or even reducing tumor volume, as many as 40% of patients still experience relapse, which accounts for more than 60% of the breast cancer-related deaths [1, 2]. Recent evidence has demonstrated that many types of cancer, including breast cancer, contain a small population of cancer stem cells (CSCs) responsible for tumor initiation, propagation and regeneration [3, 4]. Similar to adult stem cells, this minor population of cancer cells possesses the capacity to self-renew and differentiate into the heterogeneous lineages of cancer cells that comprise the tumor [5]. Moreover, preclinical studies have demonstrated that breast CSCs reside in a quiescent state, and are intrinsically more resistant to conventional cancer therapies than bulk cancer cells, hence they may survive and repopulate the tumor, resulting in cancer relapse [6-8]. With recent studies supporting the cancer stem cell hypothesis [9-11] and the overwhelming effects of breast cancer, it is of crucial importance to develop novel strategies targeting breast cancer stem cell (CSC) population in order to kill them and prevent tumor relapse.

Curcumin (diferuloylemethane) is a polyphenol derived from the ancient Asian spice turmeric, the powdered rhizome of the herb *Curcuma longa* [12]. This dietary spice has been used for generations in traditional Asian Indian medicine for the treatment of many disorders including various respiratory conditions, wound-healing, inflammation, hepatic diseases, cough, sinusitis, and certain tumors [13, 14]. Curcumin's pleiotropic activities originate from its ability to modulate many signaling molecules such as pro-inflammatory cytokines, transcriptional factors, apoptotic proteins, growth factors, receptors, multidrug resistance transporters, kinases and genes regulating cell proliferation and apoptosis [15]. To date, numerous preclinical and clinical studies have indicated the chemopreventive and chemotherapeutic potential of curcumin in a variety of cancers [16, 17]. In breast cancer, a number of *in vitro* and *in vivo* studies demonstrated curcumin's anti-proliferative, cytotoxic and anti-metastatic effects [18, 19]. Given that multiple signaling pathways are involved in tumor formation and progression curcumin possess a high therapeutic potential against cancer [20].

A growing body of experimental evidence revealed curcumin's therapeutic potential to target cancer stem cells as a downregulator of signaling pathways playing crucial roles in stem cell survival such as Wnt, Notch-1 and NFκ-B, as well as of many P-glycoproteins overexpressed on resistant cancer stem-like cells [21-24]. Recent studies by Kakarala *et al.* showed curcumin's ability to modulate self-renewal, of normal and malignant mammary stem cells, demonstrated by the inhibited mammosphere formation as well as the reduced expression of the breast stem cell marker aldehyde dehydrogenase [23].

Despite the therapeutic potential of curcumin, its clinical development has been hindered by its low potency and bioavailability resulting from poor aqueous solubility, absorption and *in vivo* stability, as well as rapid metabolism [25, 26]. In a phase I clinical trial, in patients with various precancerous lesions, oral doses of 4, 6, and 8 g curcumin daily for three months resulted in an average peak serum concentrations of only 0.51, 0.63, and 1.77 μM, respectively [27]. Therefore, the development of a drug delivery system which will solubilize curcumin in

clinically applicable concentrations, in a stable dosage form, and release it at the target site is essential for the future clinical development of this promising adjuvant anticancer agent.

To address the bioavailability issue of poorly water-soluble anti-cancer drugs, our laboratory has exploited long-circulating, sterically stabilized phospholipid nanomicelles (SSMs) as targeted drug carriers [28-31]. SSMs are composed of biocompatible, biodegradable and relatively non-toxic polyethylene glycol (PEG)-grafted phospholipids (a component of the FDA-approved product Doxil®) [32], that spontaneously self-assemble into nano-sized (~15 nm) complexes in aqueous media [33] with very low critical micellar concentration ensuring their stability upon intravenous administration and dilution [34]. As a result of their nano-size, SSMs extravasate and accumulate in tumors through enhanced permeability and retention (EPR) effect of the leaky tumor vasculature with minimum distribution to normal tissue [35, 36]. Moreover, SSMs can also be actively targeted to the tumor site by attaching specific ligands such as the vasoactive intestinal peptide (VIP), an endogenous 28 amino acid mammalian neuropeptide [37], to the distal end of their PEG chains [38]. The high affinity receptors of VIP, namely $VPAC_1$ and $VPAC_2$, are overexpressed on the surface membranes of cells of many types of tumors including breast cancer [39-41]. Previously, VIP surface-grafted SSM were used in our laboratory to promote active targeting of solubilized anticancer agents to breast cancer cells [28, 42]. On the other hand, identification of cellular targets overexpressed on the surface of breast CSC remain to be under exploited [43]. In this respect, VIP receptors stand out as promising targets given that they were found to regulate stem cell-like properties [39, 44]

In the present study, we report the development and characterization of a novel nanomicellar formulation of VIP-surface grafted, curcumin encapsulated SSM (C-SSM-VIP) that can hinder breast CSCs along with the bulk cancer cells in a safe and effective way. To this end, we investigated the potential of SSMs as nanocarriers to improve the aqueous solubility and stability of curcumin. After which the anti-cancer effect of our C-SSM formulation was evaluated on breast cancer cells as well as breast cancer stem cells *in vitro*. Most importantly, we have shown, for the first time, a significantly higher level of VIP receptor expression in the CSC population as compared to the bulk cancer cells; therefore VIP was integrated as an active targeting moiety to achieve higher anti-CSC activity.

2. Materials and Methods

2.1. Materials

1,2-Distearoyl-*sn*-glycero-3-phosphoethanolamine-*N*-methoxy-[poly(ethylene glycol); PEG M_W 2,000] (DSPE-PEG_{2000}) was obtained from LIPOID GmbH (Ludwigshafen, Germany). Curcumin (>95%) was obtained from ChromaDex (Irvine, CA). VIP was synthesized using solid-phase synthesis by Dr. Bob Lee at the Protein Research Laboratory, Research Resources Center, at the University of Illinois at Chicago. Sunbright® DSPE-PEG_{3400}-NHS [1,2-dioleoyl-*sn*-glycero-3-phosphoethanolamine-*n*-[poly(ethylene glycol)]-*N*-hydroxy succinamide; PEG M_W 3,400] was purchased from NOF Corporation (Tokyo, Japan).

MCF-7 human breast cancer cell line was obtained from American Type Culture Collection (Manassas, VA, US). Cells were cultured in Dulbecco's Modification of Eagle's Medium; DMEM from Mediatech Cellgro® (Herndon, VA) supplemented with 10% fetal bovine serum Invitrogen FBS (Carlsbad, CA) and antibiotics (penicillin 100 U/mL and streptomycin 100 mg/mL; Mediatech Cellgro®) at 37˚C in a humidified 5% CO_2 atmosphere. Tumorsphere culture

was performed in Mammocult medium supplemented with hydrocortisone and heparin obtained from StemCell technologies (Vancouver, Canada). R-Phycoerythrin (PE)-conjugated $IgG2_{aκ}$ antibody against human CD24 (CD24-PE; clone ML5), Allophycocyanin (APC)-conjugated $IgG2_{bκ}$ antibody against human CD44 (CD44-APC; clone G44-26) and corresponding mouse isotype-matched antibodies were obtained from BD Pharmingen (San Diego, CA). 5-carboxyfluorescein (FAM)-labeled VIP was from Anaspec (Fremont, CA). Vectashield® mounting medium with 4',6-diamidino-2-phenylindole (DAPI) fluorescent stain was from Vector Laboratories (Burlingame, CA). All other chemicals used were purchased from ThermoFisher Scientific (Pittsburgh, PA) or Sigma-Aldrich (St. Louis, MO).

2.2. Preparation of curcumin-loaded sterically stabilized phospholipid nanomicelles

Aqueous dispersions of C-SSM were prepared by the film rehydration/reconstitution technique as previously described in our laboratory [33]. Briefly, 1mM DSPE-PEG_{2000} and varying concentrations of curcumin (270-1085 µM or 100-400 µg/ml) were dissolved in methanol in separate vials and vortexed until complete dissolution. DSPE-PEG_{2000} and curcumin solutions were then added to round bottom flasks at appropriate ratios. Solvent was subsequently removed using a vacuum rotary evaporator (BUCHI Labortechnik AG; Flawil, Switzerland) under a stream of argon and vacuum (650 mm Hg pressure) at 55°C and 150 rpm for 30 minutes. It is worth noting that curcumin is considered to be stable at this temperature as it is usually extracted from turmeric at temperatures ranging from 50-60°C. The residual solvent from the resulting film was removed under vacuum overnight in dark. Thereafter, the dried film was rehydrated with 10 mM PBS (pH 7.4) and the resulting dispersion was vortexed until the film was dissolved, followed by bath sonication for 5 min. Flasks were then flushed with argon, sealed, and allowed to equilibrate in dark for 2 hours at 25°C to produce C-SSM. Drug-free "empty" SSM were prepared following the same procedure described above, but excluding the addition of curcumin.

For the preparation of the actively targeted formulation of curcumin-loaded VIP-surface grafted SSM (C-SSM-VIP), VIP was conjugated to the distal end of DSPE-PEG_{3400}-NHS as previously described in our laboratory [45]. This reaction takes place between NHS-ester and a primary amine yielding 1:1 DSPE-PEG_{3400}-VIP conjugate. Briefly, VIP and DSPE-PEG_{3400}-NHS were dissolved separately in cold isotonic HEPES buffer (10 mM, pH 6.6). The DSPE- PEG_{3400} solution was then added in small increments to the VIP solution at 4°C with gentle stirring to yield final concentrations of 0.3 mM VIP and 1.5 mM DSPE-PEG_{3400}-NHS. The reaction was allowed to continue at 4^{o}C for 2h and stopped by adding 5 µL of 1M glycine solution to the reaction mixture to consume the remaining NHS moieties. The DSPE PEG_{3400}-VIP conjugation was verified by SDS-PAGE electrophoresis. Thereafter, DSPE- PEG_{3400}-VIP was incorporated into preformed C-SSM dispersion in 1:4 (v/v) ratio by co-incubation at 25°C for 1 hr in the dark to obtain the final C-SSM-VIP containing ~200 µg/mL curcumin, 1 mM DSPE- PEG_{2000} and 0.06 mM VIP.

2.3. Characterization of curcumin-loaded nanomicelles

Particle size analysis

Particle size distribution and mean hydrodynamic diameters of the aqueous dispersions of empty SSM and curcumin formulations in SSM or VIP-surface grafted SSM were measured

using a dynamic light scattering (DLS) particle sizer (Agilent 7030 NICOMP DLS/ZLS, Santa Clara, CA) equipped with a 100 mW He-Ne laser (excitation at 632.8 nm) set up at a fixed scattering angle of 90° on the same day of preparation and after 3 days of storage. The mean hydrodynamic particle diameters ($\bar{d}_h$) in aqueous dispersions were obtained from the Stokes-Einstein relation using the measured diffusion of particles in solution. Measured size was presented as the average of at least three runs.

Drug content analysis

The concentration of curcumin solubilized in SSM or SSM-VIP was determined by reverse-phase HPLC (RP-HPLC). A Prominence HPLC system consists of a quaternary pump with an online degasser, auto sampler and diode array detector (Shimadzu Scientific Instrument, Inc., Tokyo, Japan). Aqueous dispersions of C-SSM or C-SSM-VIP were dissolved in methanol. 20 µL samples were injected in Zorbax 300 SB-C18 column (250 x 4.6 mm, 5 µM pore size; Agilent Technologies, Santa Clara, CA). The mobile phase was composed of methanol, water and acetonitrile (39.5 : 350 : 460, v/v/v), acidified with 0.1% trifluoroacetic acid at a flow rate of 0.75 mL/min. Absorbance was measured at 425 nm. Chromatographic peak areas were integrated by using EZStart 7.4 software

2.4. Stability of curcumin-loaded nanomicelles

Curcumin-loaded SSMs were prepared in PBS as described above at 1mM lipid and 200 µg/ml curcumin concentrations. As a control, free curcumin, at the same concentration, was dissolved in PBS containing 10% v/v methanol. The samples were incubated at 37°C in dark for 8 hours. 100 µL aliquots were withdrawn from each sample, at pre-determined time points. Aliquots were mixed with 900 µL of methanol for detection of curcumin concentrations by RP-HPLC as described above.

2.5. Scale-up and lyophilization studies

Formulations of C-SSM were prepared as described earlier, at optimized lipid/drug ratio, with curcumin concentration of 2 mg/ml in 10mM DSPE-PEG_{2000} lipid followed by characterization of particle size by DLS and curcumin concentration by RP-HPLC as described above.

C-SSM samples were lyophilized according to previously described protocols implemented by our lab for SSM [46]. Briefly, 1 mL of equilibrated C-SSM samples, without addition of a cryo- or lyoprotectants, were stored in lyophilization vials (n=3) overnight at -80°C, followed by freezing in liquid nitrogen for at least 3 min before overnight lyophilization using the Labconco FreeZone® 6 Litre FreezeDry System (Labconco, Kansas, MO). Lyophilized cakes were rehydrated with sterile water and allowed to equilibrate for 2 h at 25°C before analysis for particle size and drug content.

2.6. Cytotoxicity of curcumin-loaded SSM against MCF-7 cells

Cytotoxicity of C-SSM was evaluated on MCF-7 human breast cancer cells by sulforhodamine B assay. Briefly, 12,000 cells/well were seeded in 96-well plates and allowed to attach overnight. Cells were treated with C-SSM nanomedicine with final curcumin concentrations ranging from 25 to 100 µM (in wells). “Free” curcumin dissolved in 0.5% DMSO

in DMEM at the same concentrations (25 – 100 µM) were used as positive controls. Empty SSM at lipid concentration corresponding to the highest lipid concentration of C-SSM, as well as DMSO and PBS (pH 7.4) were used as vehicle controls. Plates were incubated for 72 h at 37°C in 5% CO_2 humidified atmosphere. Thereafter, cell viability was determined by the sulforhodamine B cytotoxicity assay as previously described [47]. Optical density (O.D.) of acetic acid fixed -sulforhodamine B-stained- cells was measured at 515 nm using Biotek Synergy™ H4 plate reader (Winooski, VT, USA). OD values from the treated samples were normalized to that of PBS treated control. The half maximal inhibitory concentration (IC_{50}) of C-SSM and free curcumin were calculated using nonlinear regression analysis based on generated curves of survival percentage vs. concentration.

2.7. Tumorsphere formation assay and treatments

Cancer stem/progenitor cells were previously shown to be enriched in tumorspheres derived from breast cancer cells, owing to the unique ability of stem cells to grow and form spherical clusters in non-adherent culturing conditions [48, 49]. Tumorsphere culture was performed as described previously by Dontu *et al* [48]. Briefly, dissociated MCF-7 cells were plated in 24-well ultra-low attachment plates (Corning Inc., Corning, NY) at a density of 15,000 viable cells/well in MammoCult®, StemCell Technologies, Vancouver, Canada) supplemented with hydrocortisone and heparin. Average sphere forming efficiency (SFE) was evaluated after 7 days of culture of primary and secondary tumorspheres under an inverted Olympus IX70 fluorescent microscope equipped with a CCD camera (Olympus, Center Valley, PA) by counting spheres that are larger than 60 µm in diameter using the ImageJ Software. For secondary tumorsphere formation, primary tumorspheres were harvested by gentle centrifugation and dissociated both enzymatically using trypsin and mechanically using a 22 gauge needle for 2 minutes. Single cell suspension was then seeded in 24-well ultra-low attachment plates (Corning, NY) at a density of 2,000 viable cells/well for a secondary tumorsphere culture.

To test the inhibitory effect of curcumin-loaded SSM on tumorsphere formation, MCF-7 cells in adherent 6-well plates were treated with freshly prepared samples of 10 µM or 20 µM C-SSM and compared to free curcumin dissolved in 0.5% DMSO in DMEM. DMSO and PBS (pH 7.4) or 20 µM empty SSM were used as vehicle controls. After 72 hours incubation, cells were triple-washed with PBS, trypsinized and seeded in ultra-low attachment plates for the tumorsphere culture. Second passage was grown in the absence of treatments. Furthermore, to test the effect of actively targeted nanomedicine to inhibit tumorsphere formation, C-SSM-VIP, C-SSM and free curcumin at 5 µM concentration, as well as PBS and DMSO controls, were incubated with the tumorsphere cultures of MCF-7 cells. The sphere forming efficiency was evaluated after 7 days of tumorsphere culture.

2.8. Flow cytometric analysis of $CD44^{+}/CD24^{-/low}$ breast cancer stem cells

The putative breast CSCs were first identified as cells isolated from primary breast tumors or mammary cell lines based on a $CD44^{+}/CD24^{-/low}$ immunophenotypical profile [50]. MCF-7 cells treated with C-SSM, free curcumin or vehicle controls for 72 hours were rinsed, dissociated enzymatically with trypsin and counted. At least $5x10^5$ cells were incubated in 100 µL antibody solution of CD24-PE and CD44-APC in PBS with 3% BSA for 10 minutes on ice

(1:3.2:20 v/v/v, respectively). Isotype-matched antibodies were used as negative controls and for gating purposes. After incubation, cells were washed by centrifugation and strained through 35-µm filter prior to sorting. The samples were analyzed for fluorescence from CD44-APC, CD24-PE and curcumin using Cyan^{TM} ADP Analyzer (Beckman Coulter Inc., Schaumburg, IL), or sorted for $CD44^{+}/CD24^{-/low}$ cancer stem cells (CSC) and $CD44^{+}/CD24^{high}$ bulk cancer cell populations using the Beckman Coulter MoFlo^{TM}. (Schaumburg, IL). Dead cells were excluded by gating for cells based on forward versus side scatter.

2.9. VIP-receptor ligand-binding analysis

MCF-7 cells were sorted using flow cytometry as prescribed in the previous section into the CSC and bulk cancer cell populations. Sorted cells were repeatedly washed with PBS by centrifugation and cytospun onto poly-L-lysine coated glass slides ($5x10^4$ cells/well) at 1000 rpm for 5 minutes using a Shendon CytoSpin Cytocentrifuge (ThermoFisher Scientific, Pittsburgh, PA) within 1 h after sorting. The resulting cell smears were allowed to air dry, followed by cell fixation with 4% paraformaldehyde for 10 min. Unspecific binding to cells was blocked by incubation in PBS with 10% FBS for 30 minutes, after which cells were stained with 0.5 µM FAM-labeled VIP in binding buffer (DMEM with 0.1% bacitracin and 50µM Pefabloc) at 37^{o}C for 1 hour. Cells auto-fluorescence was detected by cell incubation in binding buffer alone without FAM-VIP. Nonspecific binding was determined by treatment with excess unlabeled VIP (39.4 µM) followed by incubation with FAM-labeled VIP. After washing with PBS, cells were mounted with Vectashield® mounting medium containing DAPI nuclear stain. Sections were analyzed under a Carl Zeiss LSM 510 Meta confocal microscope (Carl Zeiss Microscopy, Thornwood, NY). The VIP binding to receptors on MCF-7 CSCs and bulk cancer cells were evaluated by quantifying the mean fluorescence intensities from the micrographs with the Zeiss LSM Image Browser software.

2.10. Statistical Analysis

All experiments were performed in triplicates. Data were expressed as mean ± standard deviation (SD). Two-tailed independent student's t-test and ANOVA were used to compare tested groups. Differences were considered significant when $p < 0.05$. Statistical analyses were conducted using SPSS version 17.1 and Microsoft Excel 2007.

3. Results

3.1. Characterization of curcumin-loaded SSM

To determine the maximum encapsulation efficiency of curcumin in SSM, we prepared a series of C-SSM at fixed lipid concentration of 1mM with increasing curcumin concentrations (100-400 µg/ml). Immediately after preparation, all C-SSM formulations showed mean hydrodynamic diameters ($\bar{d}_h$) ~15 nm as measured by DLS with a narrow unimodal size distribution (Fig. 1 and Table 1). However, after 3 days of incubation at 25°C, a secondary species of sterically stabilized particles (SPP) was identified upon DLS analysis of samples with curcumin concentration ≥ 250 µg/mL, and was represented as the additional peak (~200 to 500

nm) shown in Fig. 1b. In contrast, the C-SSM formulations, at drug concentration ≤ 200 µg/mL, remained stable as an aqueous dispersion over the course of a 10 days incubation period (Fig. 1d). This formulation had a mean hydrodynamic diameter of ~15.1 ± 2.7 nm (Table1) with a loading efficiency ~ 90% as measured by RP-HPLC, and was chosen as the optimum formulation to be used for further experiments.

Table 1: *Characteristics of C-SSM nanomedicine in 1mM lipid dispersion*

Loaded curcumin concentration (µg/mL)	**Particle Size (nm)***	**SSP after 3 days**
400	14.1 ± 2.4	Yes
300	15.3 ± 3.1	Yes
250	16.4 ± 2.8	Yes
200	15.1 ± 2.7	No
150	14.7 ± 3.2	No
100	14.5 ± 3.2	No
0	14.4 ± 2.4	No

3.2. Stability of curcumin-loaded SSM versus free curcumin

One of the major limitations associated with curcumin's poor bioavailability is its rapid degradation. Therefore, we evaluated the stability of curcumin as a part of our nanomedicine C-SSM. Whereas free curcumin underwent rapid degradation (>50% was degraded after 10 minutes of incubation), nanomicellar curcumin remained stable during the 8-h course of the study (Fig. 2). Thus, these results demonstrate that our C-SSM formulation remarkably increases the stability of curcumin by providing protection against hydrolytic degradation.

3.3. Scale-up and lyophilization potential of curcumin-loaded SSM

Although we have found that the short-term stability of curcumin was remarkably improved in SSM, the lyophilization potential of our formulation was further investigated to ensure the long-term stability of phospholipids [51]. We have previously found that optimal DSPE-PEG_{2000} concentration for SSM lyophilization ranged from 10-15 mM [46], therefore our current samples were prepared with 10 mM lipid concentration, keeping a similar lipid : drug ratio as our optimal formulation . Lyophilized cakes of C-SSM had an elegant appearance with slight shrinkage from the side walls of the vials; the cakes underwent complete dissolution upon reconstitution to form clear dispersions with curcumin's natural yellow color. The properties of C-SSM in terms of particle size and loading efficiency did not significantly change after freeze-drying and reconstitution (Table. 2).

Table.2: Physicochemical properties of C-SSM nanomedicine before and after lyophilization

Samples	**Particle Size (nm)***	**Loading Efficiency* (%)**
Before Freeze-Drying	11.5 ± 2.0	86.0 ± 4.8

After Freeze-Drying	12.4 ± 2.5	81.5 ± 4.6

3.4. Curcumin-loaded SSM improves the cytotoxicity of curcumin on MCF-7 cells

The in vitro anticancer activity of C-SSM formulation and free curcumin was investigated on MCF-7 breast cancer cells. The cytotoxic effect of both free curcumin and C-SSM was found to be dose-dependent (Fig. 3a), whereas vehicle controls did not show significant effect on the viability of MCF-7 cells (data not shown). However, 72 h incubation with C-SSM consistently resulted in significant reduction in cells viability as compared to free curcumin in DMSO for the tested range of concentrations (Fig. 3a). Moreover, the half maximal inhibitory concentration (IC_{50}) of C-SSM was significantly lower than that of free drug: 14.2 ± 1.2 μM vs. 26.1 ± 3.0 μM respectively (P <0.01) Fig. 3b. Therefore, these findings demonstrate that curcumin-loaded SSM exhibited comparatively better anticancer activity than free curcumin.

3.5. Curcumin-loaded SSM enhances the inhibitory effect of curcumin on MCF-7 tumorsphere formation

Recent studies have demonstrated that breast cancer stem/progenitor cells, similar to human breast stem/progenitor cells, could be enriched in floating mammospheres (also known as tumorspheres) based on their unique ability to survive in non-adherent suspension as spherical clusters [48, 49]. On the other hand, curcumin was recently demonstrated to inhibit the formation of tumorspheres from MCF-7 cells [23]. In order to determine whether the C-SSM nanomedicine could improve curcumin's efficacy to suppress tumorsphere formation, adherent MCF-7 cells were treated with C-SSM or free curcumin for 72 h, and then detached and cultured in ultra-low attachment plates for 7 days for spheres to form. As shown in (Fig. 4a), while 10 μM free curcumin did not exhibit a significant effect on tumorsphere formation, the C-SSM formulation with an equivalent dose, as well as free curcumin and C-SSM at 20 μM doses resulted in significantly lower sphere forming efficiencies compared to the PBS (pH 7.4) treated control. In addition, C-SSM, at both 10 μM and 20 μM doses, significantly inhibited tumorsphere formation in comparison to free curcumin, with sphere forming units (SFU) of 93.3 ± 11.2% vs. 62.6 ± 10.6% for 10 μM curcumin and 72.7 ± 14.4% vs. 36.0 ± 4.7% for 20 μM curcumin respectively. Furthermore, 20 μM C-SSM also reduced the sphere size by >2 folds compared to the PBS treated control (P<0.05), while free curcumin did not show significant effect on this property for the tested doses (Fig. 4b).

3.6. Curcumin-loaded SSM improves the cytotoxicity of curcumin to $CD44^{+}/CD24^{-/low}$ MCF-7 cancer stem cells

Putative cancer stem cells were first isolated from breast carcinoma based on a $CD44^{+}/CD24^{-/low}$ immune-phenotype and were found to be highly tumorigenic when injected into mice [50]. In an attempt to evaluate whether C-SSM could improve the cytotoxicity of curcumin against $CD44^{+}/CD24^{-/low}$ breast CSCs, we treated MCF-7 cells with C-SSM or free curcumin for 72 hours and analyzed the drug uptake as well as the change in the percentage of the CSC population. Taking advantage of curcumin's intrinsic fluorescence, the uptake of curcumin by

$CD44^+/CD24^{-/low}$ CSCs and $CD44^+/CD24^{high}$ bulk cancer cells was quantified by flow cytometry (Fig. 5a).

We found that nanomicellar curcumin at 10 µM curcumin concentration increased the drug internalization into bulk cancer cells by 6.4-fold and into CSCs by 3.5-fold ($P<0.05$) compared to free curcumin. Likewise, 20 µM C-SSM also increased curcumin uptake by 2.8-fold in bulk cancer cells, and by 1.8-fold in CSCs compared to free curcumin in a dose response manner. Our data are in agreement with the results of the study by Mohanty and Sahoo, where it was reported that the cellular uptake of the curcumin encapsulated in glycerol monooleate and pluronic F-127 nanoparticles was higher than that of free curcumin with the same treatment concentration [52].

We also investigated whether this increased cellular uptake of nanomicellar curcumin resulted in a higher inhibition of $CD44^+/CD24^{-/low}$ CSCs from MCF-7 cells also. As shown in Fig. 6b and c, among all the treatment groups, only 20 µM C-SSM significantly decreased the percentage of $CD44^+CD24^{-/low}$ CSC population compared to the PBS control (56% decrease, $P < 0.05$). It is worth mentioning that at the 20 µM dose, nanomicellar curcumin was able to inhibit the viability of MCF-7 cells by 70% (Fig. 3), while reducing the proportion of $CD44^+CD24^{-/low}$ CSCs by more than 2-fold (Fig. 5b). These findings indicate that nanomicellar curcumin shows cytotoxicity to both bulk tumor cells and CSCs with more preferential specificity for the CSC population. Taken together, these findings suggest that the C-SSM formulation improves the in-vitro efficacy of curcumin against both bulk breast cancer cells and breast CSCs.

3.7. MCF-7 cancer stem cells overexpress VIP receptors

Identification of cellular targets overexpressed on the surface of CSCs holds great significance for developing nanomedicine that can be actively targeted to these resistant cells. Yet there are currently only a few potential CSC markers exploited for targeting purposes [44]. In this respect, VIP receptors stand out as promising targets, given that these receptors are overexpressed in many types of cancers (including breast cancer) and that they regulate stem cell-like properties [33, 45]. Therefore, we evaluated the expression of VIP receptors on CSCs isolated from MCF-7 cells, with the aim of identifying a novel molecular target to be employed in developing active targeting strategies to these resistant cells. We quantified and compared the mean fluorescence intensities (MFIs) from $CD44^+/CD24^{-/low}$ cancer stem cell and $CD44^+/CD24^{high}$ bulk cancer cell populations stained with fluorescence-labeled VIP. The specificity of the ligand-binding assay was confirmed by the low average MFI of the nonspecific binding control (data not shown). As shown in (Fig. 6 a and b), $CD44^+/CD24^{-/low}$ breast CSC population had a ~3 times higher expression of the VIP receptors compared to that of $CD44^+/CD24^{high}$ bulk breast cancer cells ($P < 0.05$). The green fluorescence was found to be more difused and spread out through the cells (Fig. 6b) as VIP receptors are found to be expressed on the nuclear membranes as well as plasma membrane of breast cancer cells [53]. Furthermore, VIP is believed to increase its own intracellular and extracellular levels, and could be involved in the regulation of VPAC(1)-receptor traffic from the plasma membrane to the nucleus, and this would explain the diffusion of green fluorescence throughout the cells. These promising preliminary results indicate that VIP receptors are overexpressed in the CSC population of MCF-7 cells compared to the bulk cancer cells, thus revealing the potential of

active targeting through these receptors as a means to increase cell selectivity and uptake. Although further experiments, such as western blotting, are required to confirm our findings

3.8. Characterization of VIP-surface grafted SSM loaded with curcumin

Previous *in vitro* and *in vivo* work from our laboratory has demonstrated that active targeting through VIP receptors with VIP-surface grafted SSM significantly improves the potency of cytotoxic agents [30, 42]. Therefore, we intend to improve the efficacy of C-SSM against CSCs by developing a novel VIP-surface grafted formulation of C-SSM to actively target the VIP receptors. VIP was successfully conjugated to DSPE-PEG_{3400}-NHS which was confirmed by SDS-PAGE electrophoresis (data not shown). The prepared DSPE-PEG_{3400}-VIP was incubated with the C-SSM stock dispersion to achieve physical incorporation. The resulting VIP-surface grafted curcumin nanomicellar (C-SSM-VIP) showed a unimodal particle size distribution with $\bar{d}_h$ of 17.2 ± 0.5 nm, indicating self-association of curcumin with SSM-VIP (Fig. 7). The loading efficiency of the C-SSM-VIP formulation was around 88.4 ± 2.1 % as determined by RP-HPLC.

3.9. Curcumin-loaded SSM actively targeted to VIP receptors further enhance the inhibitory effect of curcumin on MCF-7 Tumorspheres

To determine whether the VIP targeted curcumin nanomicellar would further improve the anti-CSC activity of curcumin, single cell suspensions of MCF-7 cells were treated in the tumorsphere culture with different formulations and sphere forming efficiencies were evaluated after 7 days. As shown in (Fig. 8), 5 µM VIP-surface grafted C-SSM had a significantly higher inhibitory effect on tumorsphere formation than both free curcumin and C-SSM ($P < 0.05$). This finding indicates the contribution of receptor-mediated particle internalization on increasing the overall cellular uptake of curcumin, leading to an amplified activity of the drug to inhibit tumorsphere formation.

Overall, these results indicated that VIP receptor-targeted delivery of curcumin-loaded nanomicelles further improves the anti-CSC activity of curcumin, thus demonstrating the feasibility of employing an active targeting strategy through the overexpressed VIP receptors for delivering CSC therapies.

4. Discussion

A new paradigm has emerged in recent years, revealing that cancers are initiated and sustained by a small sub-population of cells of CSC displaying properties similar to tissue-specific stem cells such as self-renewal and differentiation [9]. Accumulating evidence over the years indicated that CSCs are intrinsically more resistant to therapy than bulk cancer cells, and therefore may be responsible for tumor relapse and metastasis [54]. In this respect, naturally occurring dietary compounds have been the recent focus of CSC research, as they can modulate self-renewal pathways crucial for CSC survival. Among these compounds, curcumin, has recently been demonstrated to inhibit breast CSCs [23]. However, despite its vast potential to effectively target not only the bulk of the tumor but also the more resistant cancer stem cell population, its usefulness is limited by its poor bioavailability [25, 26]. In this study we address

these issues by developing a lipid-based nanomedicine of curcumin in sterically stabilized phospholipid micelles (C-SSM) and investigate its effectiveness on the CSC population.

The physicochemical properties of our optimized curcumin-loaded SSM formulation, specifically their reproducible and small particle size (Fig.1) make them advantageous for passive targeting to tumor tissues via the enhanced permeability and retention (EPR) effect as well as for providing deeper penetration into the tumor interstitium [55]. Another advantage is that our SSM carriers offer protection of drugs from degradation (Fig.2) potentially improving drug stability. In addition to a satisfactory short-term stability, our Nano-particulate formulation possesses the capacity to withstand long-term storage conditions upon lyophilization. It is also worth noting that at the lipid concentration of 15 mM, curcumin's solubility reached a level of ~ 2.6 mg/mL, corresponding to a ~$2.4x10^5$ folds increase to its previously reported maximum aqueous solubility of 11 ng/mL [56].

Numerous preclinical studies have shown curcumin's cytotoxic effect on breast cancer cells [16, 18, 19]. Our results support these findings demonstrating the efficacy of curcumin in inhibiting the survival of MCF-7 cells in a dose dependent manner (Fig. 3a). We also found that the cytotoxicity of curcumin in SSM was remarkably improved compared to that of free drug (Fig. 3b), this could be partially attributable to the efficient protection of the drug inside the hydrophobic core of SSM. This, in turn, would allow a greater amount of curcumin to remain intact for 72 hours and exert its cytotoxic effect. On the other hand, based on the findings of Kakarala et al. [23], showing curcumin's potential to hinder breast cancer stem cells; we evaluated the *in vitro* anti-CSC activity of our curcumin nanomicellar formulation. Pre-treatment of MCF-7 cells with either free or nanomicellar curcumin (10 and 20 µM) was found to significantly suppress the tumorsphere formation in a dose-dependent manner (Fig. 4), indicating curcumin's capacity to eliminate the tumorsphere-initiating breast CSCs

Although SSM nanocarriers significantly improved the accumulation of curcumin inside both bulk and CSCs (Fig. 5a), with the 20 µM C-SSM nanomedicine resulting in 56% decrease in CSCs population (Fig. 5b), the inhibitory effect of 10 µM C-SSM demonstrated in the tumorsphere assay was not observed on the percentage of CSC population. One possible explanation is the discrepancies between the two methods. While the flow cytometric analysis of the $CD44^+/CD24^{-/low}$ is a measure of the surviving CSC population after treatment, the tumorsphere formation assay is a measure of both the number of surviving CSCs and their impaired proliferative capacity. Therefore, it is likely that C-SSM, at a lower 10 µM curcumin dose, inhibits tumorsphere formation by impairing the proliferative capacity of CSCs.

As we evaluated the level of VIP receptor expression on CSCs isolated from the MCF-7 cell line, our results demonstrated that the VIP receptors were overexpressed by approximately 3-fold in the $CD44^+/CD24^{-/low}$ CSC population compared to the $CD44^+/CD24^{high}$ bulk cancer cells (Fig. 6). These data were indicative of the potential of active targeting of breast CSCs through VIP receptors to increase the *in vivo* cell specificity, while maximizing drug accumulation inside these cells. However, further studies are necessary to determine whether the VIP receptors are also differentially expressed between the CSC and bulk cancer cell populations of other breast cancer cell lines as well as primary breast carcinoma tissues.

The physicochemical properties of C-SSM-VIP nanomedicine, similar to C-SSM, had a unimodal particle size distribution (Fig. 7), a high loading efficiency, and a significant tumorsphere inhibitory effect obtained with 5 µM C-SSM-VIP treatment compared to C-SSM

(Fig.8). These findings provide evidence for the contribution of receptor-mediated internalization to the overall cellular uptake of curcumin.

Overall, our study provides a novel strategy for the effective elimination of breast cancer cells along with CSCs. As a breast cancer nanomedicine, C-SSM-VIP possesses the combined advantages of i) curcumin, as a dietary compound with no observed toxicity and a vast chemotherapeutic potential, ii) sterically stabilized, biocompatible and biodegradable phospholipid nanomicelles as a safe delivery system that provides protection and increases the potency of curcumin, and iii) active targeting of VIP receptors overexpressed on breast CSCs as a means to increase cell selectivity and intracellular drug uptake. Hence, our findings demonstrate the proof-of-concept that CSC therapies could be more efficiently delivered through active targeting of the VIP receptors with the VIP-grafted SSM nannocarrier. However, further studies are needed to show the potential of the nanomicellar formulations to improve the *in vivo* chemotherapeutic activity of curcumin.

5. Conclusion

In conclusion, we found that the encapsulation of curcumin in sterically stabilized micelles (C-SSM) remarkably improved curcumin's aqueous solubility and stability. This protective action of nanomicelles was confirmed by an *in vitro* cytotoxicity study, on MCF-7 breast cancer cells, showing a significantly enhanced anticancer activity for nanomicellar curcumin compared to free curcumin. More importantly, our study showed that the C-SSM nanomedicine was also able to target the resistant breast CSC population with a higher efficacy than free curcumin as determined by the tumorsphere formation assay, cellular uptake studies and the flow cytometric analysis of the $CD44^{+}/CD24^{-/low}$ CSC population. Furthermore, for the first time, VIP receptors were identified as an attractive molecular target overexpressed on breast CSCs, although further experiments, such as western blotting, are required to confirm our findings. An actively targeted nanomicellar formulation of curcumin, C-SSM-VIP was successfully prepared and characterized. The proof-of-concept that the anti-CSC activity of nanomicellar curcumin could further be improved by active targeting of the VIP receptors was demonstrated by the tumorsphere formation assay. Thus, these findings suggest that the SSM nanocarriers are promising carriers for the development of an injectable formulation of curcumin with a high potential to overcome its bioavailability issues and improve its efficacy against not only breast cancer cells, but also the resistant breast CSCs. The present study also provides a novel active targeting strategy, based on G-protein coupled receptors, for eradicating breast cancer cells along with CSCs in a safe and efficacious way that could potentially lead to a relapse-free treatment of breast cancer.

6. Acknowledgements

We thank Dr. Gemeinhart's laboratory for use of the microscope equipment, and Dr. Lee, the director of protein research laboratory at UIC-RRC for VIP-peptide synthesis. This study was supported in part by, NIH R01 CA121797. This investigation was conducted in a facility constructed with support from the NIH National center for Research Resources grant C06RR15482. The authors declare that no conflict of interest exists in any part of this study.

7. References

(1) Gerber B, Freund M, Reimer T. Recurrent breast cancer: Treatment strategies for maintaining and prolonging good quality of life. Dtsch Arztebl Int. 2010;107:85-91.
(2) Di Cosimo S, Baselga J. Targeted therapies in breast cancer: Where are we now? Eur J Cancer. 2008;44:2781-90.
(3) Frank NY, Schatton T, Frank MH. The therapeutic promise of the cancer stem cell concept. J Clin Invest. 2010;120:41-50.
(4) Reya T, Morrison SJ, Clarke MF, Weissman IL. Stem cells, cancer, and cancer stem cells. Nature. 2001;414:105.
(5) Clarke MF, Dick JE, Dirks PB, Eaves CJ, Jamieson CH, Jones DL, Visvader J, Weissman IL, Wahl GM. Cancer stem cells--perspectives on current status and future directions: AACR workshop on cancer stem cells. Cancer Res. 2006;66:9339-44.
(6) Phillips TM, McBride WH, Pajonk F. The response of CD24(-/low)/CD44+ breast cancer-initiating cells to radiation. J Natl Cancer Inst. 2006;98:1777-85.
(7) Li X, Lewis MT, Huang J, Gutierrez C, Osborne CK, Wu MF, Hilsenbeck SG, Pavlick A, Zhang X, Chamness GC, Wong H, Rosen J, Chang JC. Intrinsic resistance of tumorigenic breast cancer cells to chemotherapy. J Natl Cancer Inst. 2008;100:672-9.
(8) Gupta PB, Onder TT, Jiang G, Tao K, Kuperwasser C, Weinberg RA, Lander ES. Identification of selective inhibitors of cancer stem cells by high-throughput screening. Cell. 2009;138:645-59.
(9) Chen J., Li Y., Yu T.-S., McKay R.M., Kernie S.G., Parada L.F., Burns D.K. A restricted cell population propagates glioblastoma growth after chemotherapy. Nature. 2012;488:522-6.
(10) Driessens G, Beck B, Caauwe A, Simons BD, Blanpain C. Defining the mode of tumour growth by clonal analysis. Nature. 2012;488:527-30.
(11) Schepers AG, Snippert HJ, Stange DE, van den Born M, van Es JH, van de Wetering M, Clevers H. Lineage tracing reveals Lgr5+ stem cell activity in mouse intestinal adenomas. Science. 2012;337:730-5.
(12) Aggarwal BB, Surh Y,Shishodia S. Advances in Experimental Medicine and Biology:The molecular targets and therapeutic uses of curcumin in health and disease. eBook. New York, NY: Springer; 2007.
(13) López-Lázaro M. Anticancer and carcinogenic properties of curcumin: Considerations for its clinical development as a cancer chemopreventive and chemotherapeutic agent. Molecular Nutrition & Food Research. 2008;52:103-27.
(14) Goel A, Aggarwal BB. Curcumin, the golden spice from indian saffron, is a chemosensitizer and radiosensitizer for tumors and chemoprotector and radioprotector for normal organs. Nutr Cancer. 2010;62:919-30.
(15) Gupta SC, Patchva S, Aggarwal BB. Therapeutic roles of curcumin: Lessons learned from clinical trials. AAPS J. 2013;15:195-218.
(16) Anand P, Sundaram C, Jhurani S, Kunnumakkara AB, Aggarwal BB. Curcumin and cancer: An “old-age” disease with an “age-old” solution. Cancer Lett. 2008;267:133-64.
(17) Dhillon N, Aggarwal BB, Newman RA, Wolff RA, Kunnumakkara AB, Abbruzzese JL, Ng CS, Badmaev V, Kurzrock R. Phase II trial of curcumin in patients with advanced pancreatic cancer. Clin Cancer Res. 2008;14:4491-9.
(18) Bachmeier B, Nerlich AG, Iancu CM, Cilli M, Schleicher E, Vené R, Dell'Eva R, Jochum M, Albini A, Pfeffer U. The chemopreventive polyphenol curcumin prevents hematogenous breast cancer metastases in immunodeficient mice. Cell Physiol Biochem. 2007;19:1-4.
(19) Aggarwal BB, Shishodia S, Takada Y, Banerjee S, Newman RA, Bueso-Ramos CE, Price JE. Curcumin suppresses the paclitaxel-induced nuclear factor-kappaB pathway in breast

cancer cells and inhibits lung metastasis of human breast cancer in nude mice. Clin Cancer Res. 2005;11:7490-8.
(20) Hanahan D, Weinberg R. Hallmarks of cancer: The next generation. Cell. 2011;144:646-74.
(21) Yu Y, Kanwar SS, Patel BB, Nautiyal J, Sarkar FH, Majumdar AP. Elimination of colon cancer stem-like cells by the combination of curcumin and FOLFOX. Translational Oncology. 2009;2:321-8.
(22) Fong D, Yeh A, Naftalovich R, Choi TH, Chan MM. Curcumin inhibits the side population (SP) phenotype of the rat C6 glioma cell line: Towards targeting of cancer stem cells with phytochemicals. Cancer Lett. 2010;293:65-72.
(23) Kakarala M, Brenner DE, Korkaya H, Cheng C, Tazi K, Ginestier C, Liu S, Dontu G, Wicha MS. Targeting breast stem cells with the cancer preventive compounds curcumin and piperine. Breast Cancer Res Treat. 2010;122:777-85.
(24) Lim KJ, Bisht S, Bar EE, Maitra A, Eberhart CG. A polymeric nanoparticle formulation of curcumin inhibits growth, clonogenicity and stem-like fraction in malignant brain tumors. Cancer Biology & Therapy. 2011;11:464-73.
(25) Anand P, Kunnumakkara AB, Newman RA, Aggarwal BB. Bioavailability of curcumin: Problems and promises. Mol Pharm. 2007;4:807-18.
(26) Bansal SS, Goel M, Aqil F, Vadhanam MV, Gupta RC. Advanced drug delivery systems of curcumin for cancer chemoprevention. Cancer Prev Res (Phila). 2011;4:1158-71.
(27) Cheng AL, Hsu CH, Lin JK, Hsu MM, Ho YF, Shen TS, Ko JY, Lin JT, Lin BR, Ming-Shiang W, Yu HS, Jee SH, Chen GS, Chen TM, Chen CA, Lai MK, Pu YS, Pan MH, Wang YJ, Tsai CC, Hsieh CY. Phase I clinical trial of curcumin, a chemopreventive agent, in patients with high-risk or pre-malignant lesions. Anticancer Res. 2001;21:2895-900.
(28) Önyüksel H, Mohanty PS, Rubinstein I. VIP-grafted sterically stabilized phospholipid nanomicellar 17-allylamino-17-demethoxy geldanamycin: A novel targeted nanomedicine for breast cancer. Int J Pharm. 2009;365:157-61.
(29) Krishnadas A, Rubinstein I, Onyuksel H. Sterically stabilized phospholipid mixed micelles: In vitro evaluation as a novel carrier for water-insoluble drugs. Pharm Res. 2003;20:297-302.
(30) Koo OM, Rubinstein I, Onyuksel H. Actively targeted low-dose camptothecin as a safe, long-acting, disease-modifying nanomedicine for rheumatoid arthritis. Pharm Res. 2011;28:776-87.
(31) Lim SB, Rubinstein I, Sadikot RT, Artwohl JE, Önyüksel H. A novel peptide nanomedicine against acute lung injury: GLP-1 in phospholipid micelles. Pharm Res. 2011;28:662-72.
(32) Working PK, Dayan AD. Pharmacological-toxicological expert report. CAELYX. (stealth liposomal doxorubicin HCl). Hum Exp Toxicol. 1996;15:751-85.
(33) Vukovic L, Khatib FA, Drake SP, Madriaga A, Brandenburg KS, Kral P, Onyuksel H. Structure and dynamics of highly PEG-ylated sterically stabilized micelles in aqueous media. J Am Chem Soc. 2011;133:13481-8.
(34) Ashok B, Arleth L, Hjelm RP, Rubinstein I, Onyüksel H. In vitro characterization of PEGylated phospholipid micelles for improved drug solubilization: Effects of PEG chain length and PC incorporation. J Pharm Sci. 2004;93:2476-87.
(35) Peer D, Karp JM, Hong S, Farokhzad OC, Margalit R, Langer R. Nanocarriers as an emerging platform for cancer therapy. Nature Nanotechnology. 2007;2:751-60.
(36) Matsumura Y, Maeda H. A new concept for macromolecular therapeutics in cancer chemotherapy: Mechanism of tumoritropic accumulation of proteins and the antitumor agent smancs. Cancer Res. 1986;46:6387-92.
(37) Laburthe M, Couvineau A, Tan V. Class II G protein-coupled receptors for VIP and PACAP: Structure, models of activation and pharmacology. Peptides. 2007;28:1631-9.

(38) Onyukse H ,Banerjee A. Phospholipid-based nanomicelles in cancer nanomedicine. In: Hunter RJ,Preedy VR. Nanomedicine in health and disease. Boca Raton, FL; Jersey, British Isles; Enfield, N.H.: CRC Press ; Science Publishers; 2011. pp.314-35.
(39) Reubi JC, Läderach U, Waser B, Gebbers JO, Robberecht P, Laissue JA. Vasoactive intestinal peptide/pituitary adenylate cyclase-activating peptide receptor subtypes in human tumors and their tissues of origin. Cancer Res. 2000;60:3105-12.
(40) Dagar S, Sekosan M, Rubinstein I, Onyüksel H. Detection of VIP receptors in MNU-induced breast cancer in rats: Implications for breast cancer targeting. Breast Cancer Res Treat. 2001;65:49-54.
(41) Gespach C, Bawab W, de Cremoux P, Calvo F. Pharmacology, molecular identification and functional characteristics of vasoactive intestinal peptide receptors in human breast cancer cells. Cancer Res. 1988;48:5079-83.
(42) Onyuksel H, Jeon E, Rubinstein I. Nanomicellar paclitaxel increases cytotoxicity of multidrug resistant breast cancer cells. Cancer Lett. 2009;274:327-30.
(43) Schatzlein AG, Cancer Stem Cells: Opportunities for Novel Diagnostics and Drug Discovery. Delivering cancer stem cell therapies - A role for nanomedicines? Eur J Cancer. 2006;42:1309-15.
(44) Callihan P, Mumaw J, Machacek DW, Stice SL, Hooks SB. Regulation of stem cell pluripotency and differentiation by G protein coupled receptors. Pharmacol Ther. 2011;129:290-306.
(45) Dagar S, Sekosan M, Lee BS, Rubinstein I, Önyüksel H. VIP receptors as molecular targets of breast cancer: Implications for targeted imaging and drug delivery. J Controlled Release. 2001;74:129-34.
(46) Lim SB, Rubinstein I, Onyuksel H. Freeze drying of peptide drugs self-associated with long-circulating, biocompatible and biodegradable sterically stabilized phospholipid nanomicelles. Int J Pharm. 2008;356:345-50.
(47) Vichai V, Kirtikara K. Sulforhodamine B colorimetric assay for cytotoxicity screening. Nat Protoc. 2006;1:1112-6.
(48) Dontu G, Abdallah WM, Foley JM, Jackson KW, Clarke MF, Kawamura MJ, Wicha MS. In vitro propagation and transcriptional profiling of human mammary stem/progenitor cells. Genes. Dev. 2003;1253-1270.
(49) Ponti D, Costa A, Zaffaroni N, Pratesi G, Petrangolini G, Coradini D, Pilotti S, Pierotti MA, Daidone MG. Isolation and in vitro propagation of tumorigenic breast cancer cells with stem/progenitor cell properties. Cancer Res. 2005;65:5506-11.
(50) Al-Hajj M, Wicha MS, Benito-Hernandez A, Morrison SJ, Clarke MF. Prospective identification of tumorigenic breast cancer cells. Proc Natl Acad Sci. 2003;100(7):3983-3988.
(51) Koo OM, Rubinstein I, Onyuksel H. Camptothecin in sterically stabilized phospholipid micelles: A novel nanomedicine. Nanomedicine. 2005;1:77-84.
(52) Mohanty C, Sahoo SK. The in vitro stability and in vivo pharmacokinetics of curcumin prepared as an aqueous nanoparticulate formulation. Biomaterials. 2010;31:6597-611.
(53) Valdehita A, Bajo AM, Fernandez-Martinez AB, Arenas MI, Vacas E, Valenzuela P, Ruiz-Villaespesa A, Prieto JC, Carmena MJ. Nuclear localization of vasoactive intestinal peptide (VIP) receptors in human breast cancer. Peptides. 2010;31:2035-45.
(54) Singh A, Settleman J. EMT, cancer stem cells and drug resistance: An emerging axis of evil in the war on cancer. Oncogene. 2010;29:4741-51.
(55) Jain RK, Stylianopoulos T. Delivering nanomedicine to solid tumors. Nat Rev Clin Oncol. 2010;7:653-64.
(56) Tonnesen HH, Masson M, Loftsson T. Studies of curcumin and curcuminoids. XXVII. cyclodextrin complexation: Solubility, chemical and photochemical stability. Int J Pharm. 2002;244:127-35.

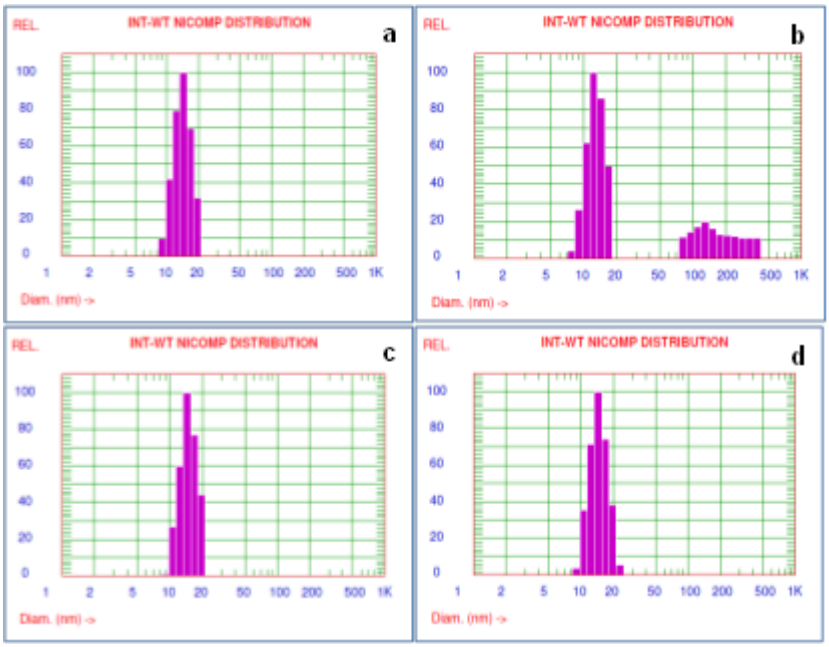

Fig.1 Representative intensity-weighted particle size distribution of C-SSM formulations (a) 250 µg/ml curcumin loaded in 1mM SSM showing unimodal size distribution on day 0, (b) 250 µg/ml curcumin loaded in 1mM SSM showing drug precipitate after 3 days of incubation, (c) 200 µg/ml curcumin loaded in 1mM SSM on day 0 and (d) 200 µg/ml curcumin loaded in 1mM SSM after 3 days of incubation

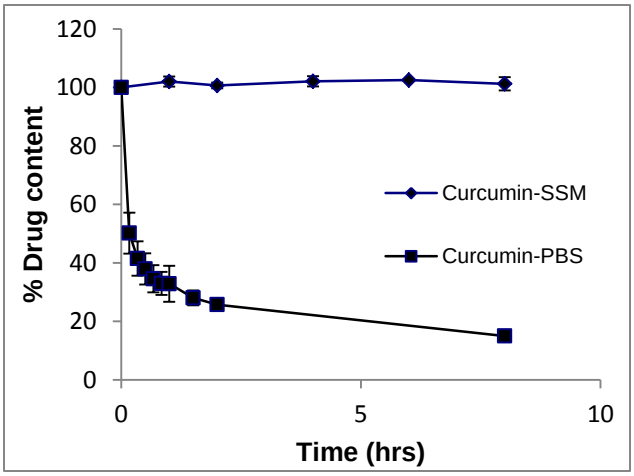

Fig.2 Stability of curcumin - SSM nanomedicine as compared to free curcumin represented by % drug content of the originally prepared samples. Experiment was performed over a period of 8 hours after incubation in 0.01 M phosphate buffered saline at 37°C. Data are mean ± SD of n=3

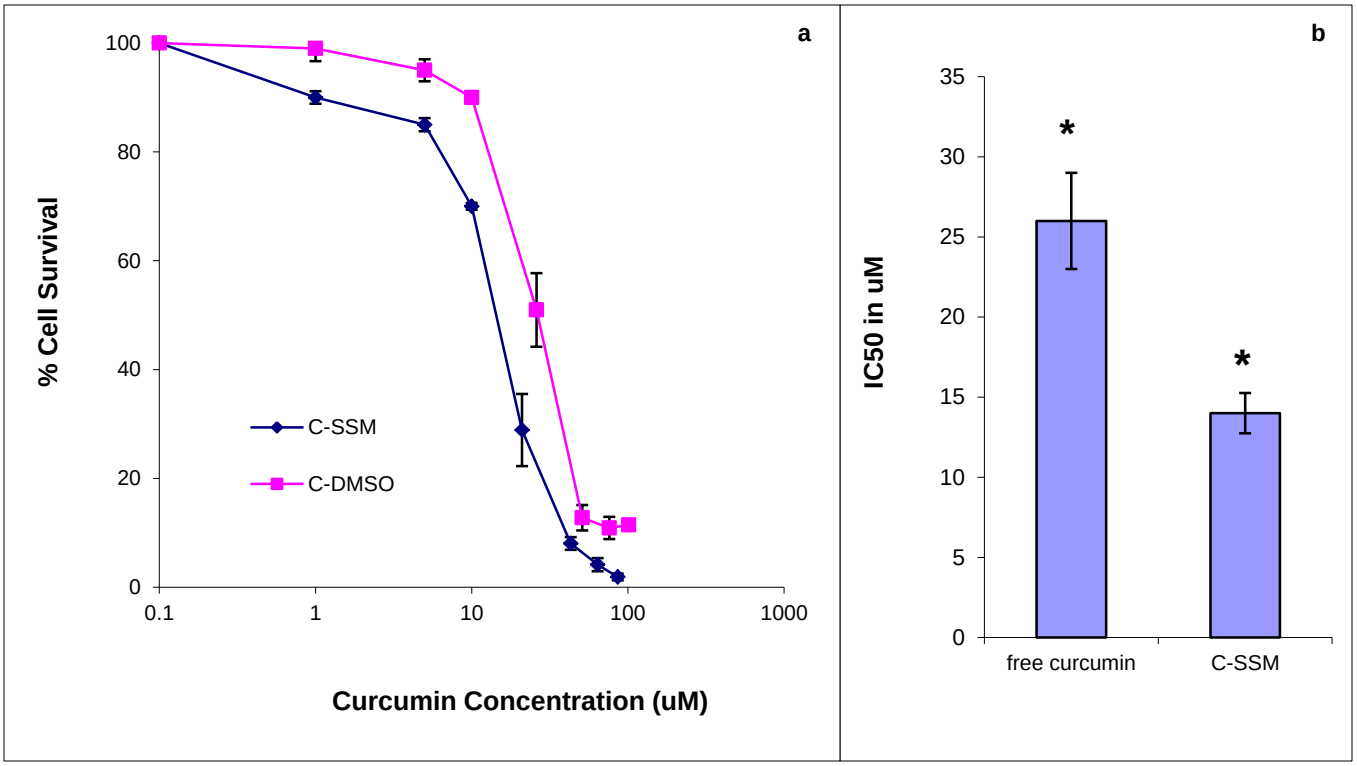

Fig.3 Curcumin formulations cytotoxicity represented by (a) % cell survival of MCF-7 breast cancer cells after treatment with (■) Curcumin in DMSO or (◆) C-SSM for 72 hrs as determined by sulforhodamine B assay. (b) IC_{50} of free curcumin and C-SSM. Results were normalized to vehicle treated controls and represented as mean ± SD of n=3, * $p < 0.05$.

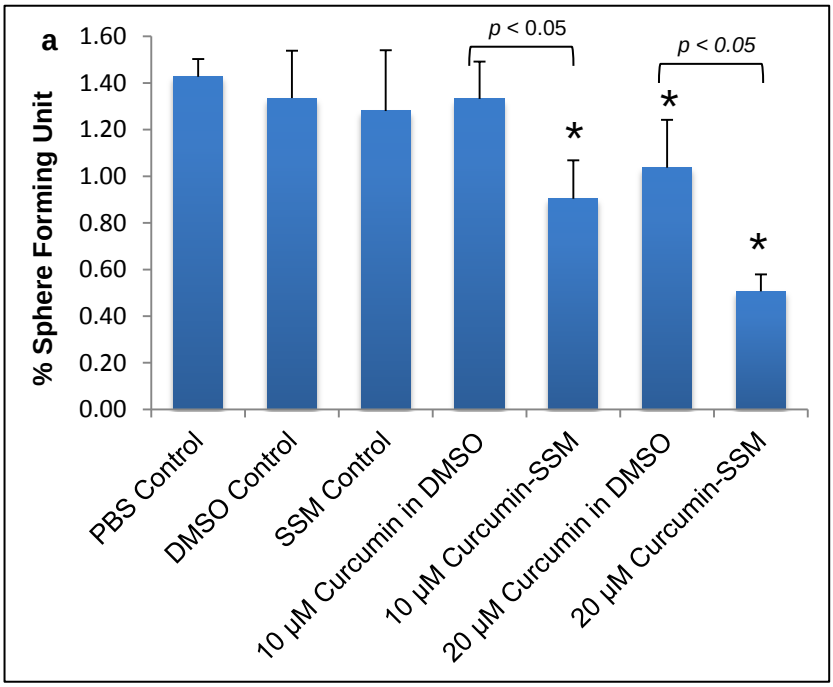

b. Tumorsphere size

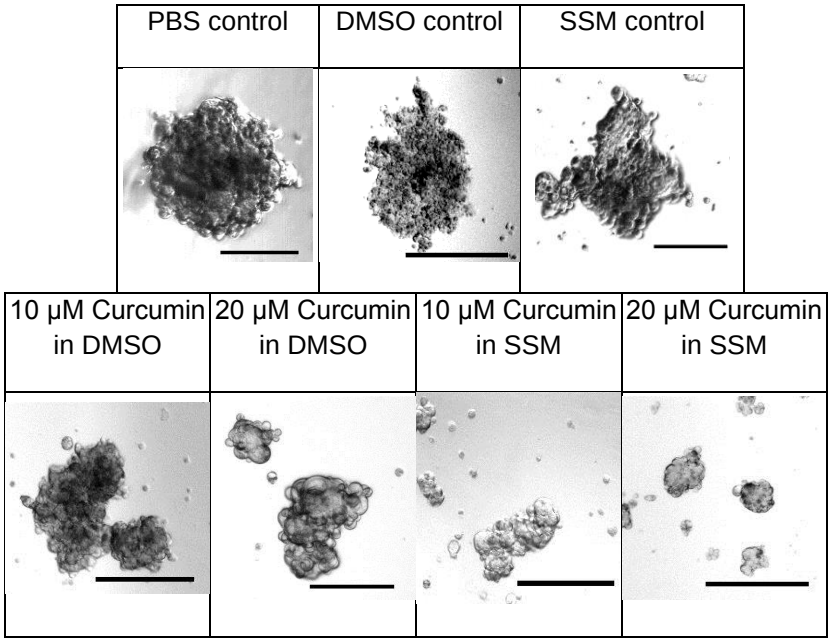

Fig. 4 Tumorsphere formation (a) Effect of different treatments on tumorsphere forming efficiency of MCF-7 cells. Cells were pre-treated with different formulations for 72 hours in adherent conditions then cultured for 7 days in tumorsphere forming conditions. * $p < 0.05$ compared to PBS treated control. Data are mean ± SD of n=3. (b) Representative images of tumorshperes illustrating the effect of different treatments on sphere size. Bar represents 50µm.

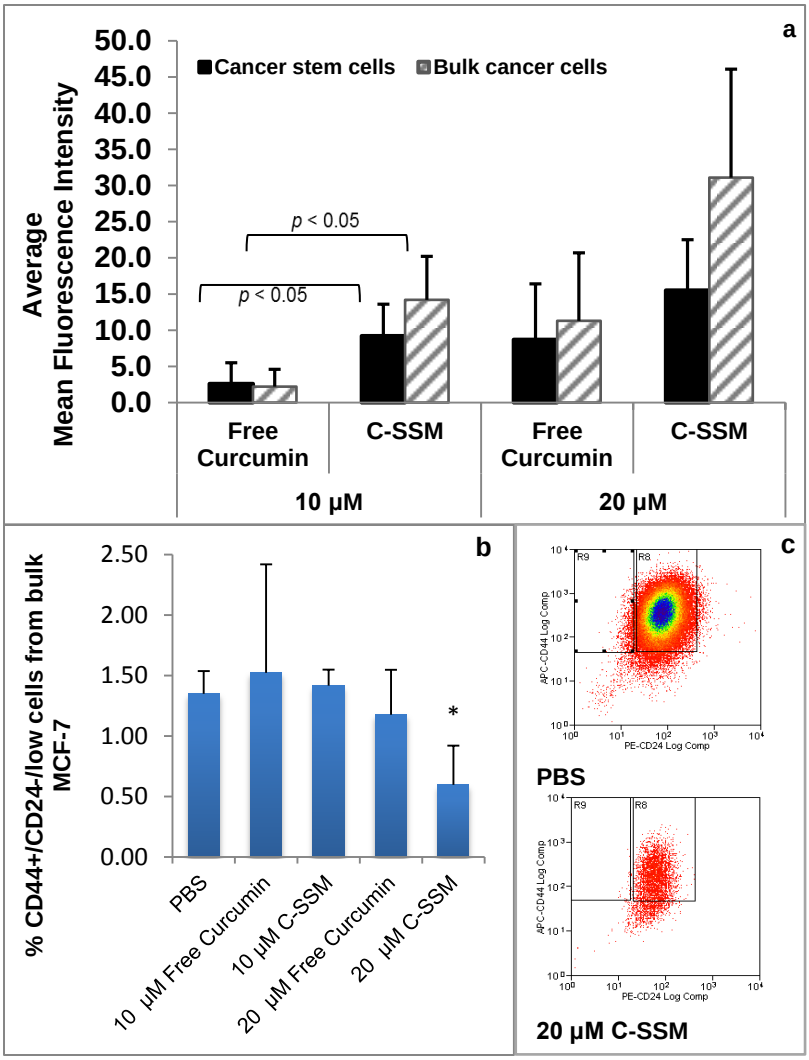

Fig. 5 The effect of free curcumin vs C-SSM on $CD44^{+}/CD24^{-/low}$ CSC and $CD44^{+}/CD24^{high}$ bulk MCF-7 population by flow cytometry. (a) SSM nanocarriers significantly increase the cellular uptake of drug cargo by both CSC and bulk cancer cells. (b) The effect of different treatments on the percentage of $CD44^{+}/CD24^{-/low}$ CSC from the overall bulk population. 20µM C-SSM significantly decreases CSC population, * $p < 0.05$ compared to PBS treated control. (c) Representative flow cytometry dot plots. Data are mean ± SD of n=4

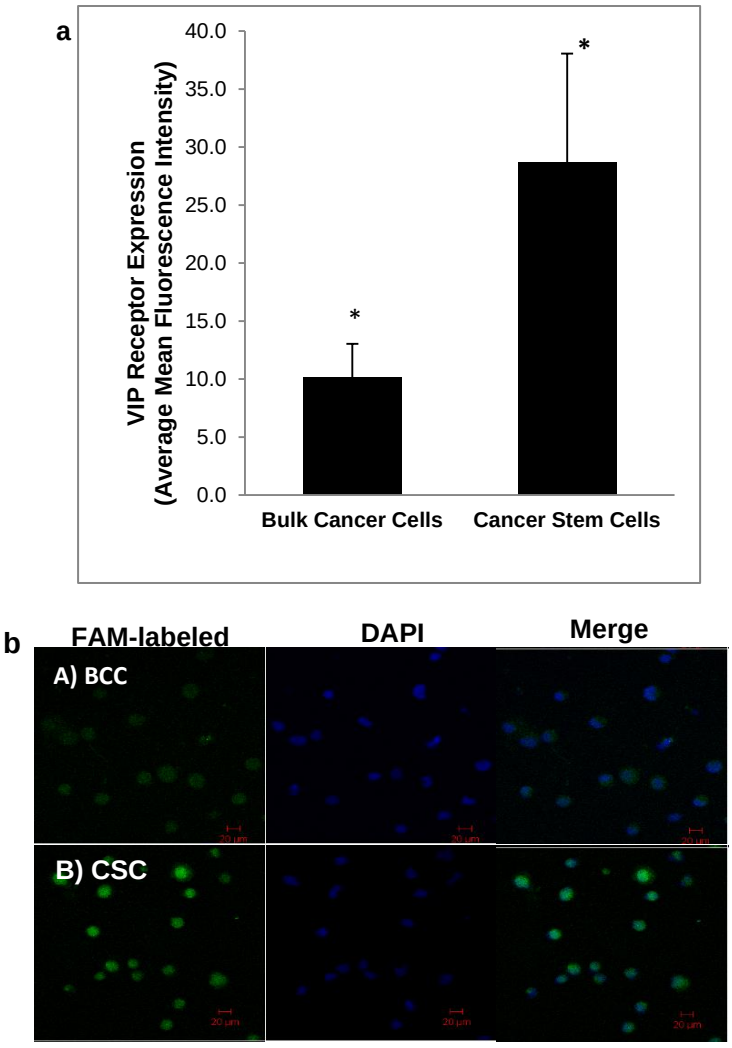

Fig. 6 VIP expression (a) the average mean fluorescence intensities of bulk cancer cells $CD44^{+}/CD24^{high}$ and cancer stem cells $CD44^{+}/CD24^{-/low}$ from MCF-7 cell line, stained with FAM-labeled VIP. * $p < 0.05$. Data are mean ± SD of n=3 representing VIP receptor expression in the two populations. (b) Confocal microscopy images showing VIP receptor expression in CSC population compared to bulk cancer cells. MCF-7 cells stained with FAM-labeled VIP (green) and DAPI (blue nuclear stain).

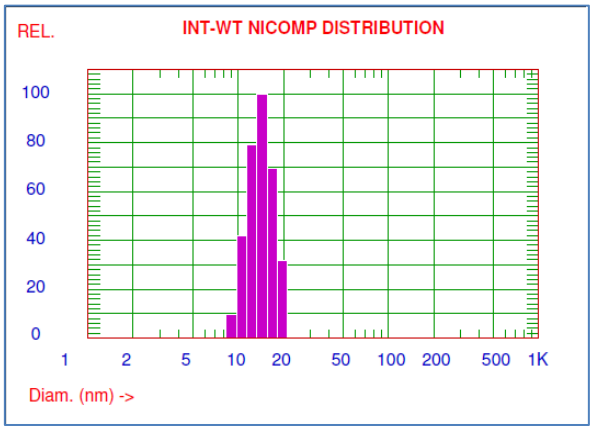

Fig. 7 Representative intensity-weighted particle size distribution of VIP-grafted curcumin nanomicellular formulation showing unimodular size distribution with mean particle diameter of 17.2 ± 0.5nm.

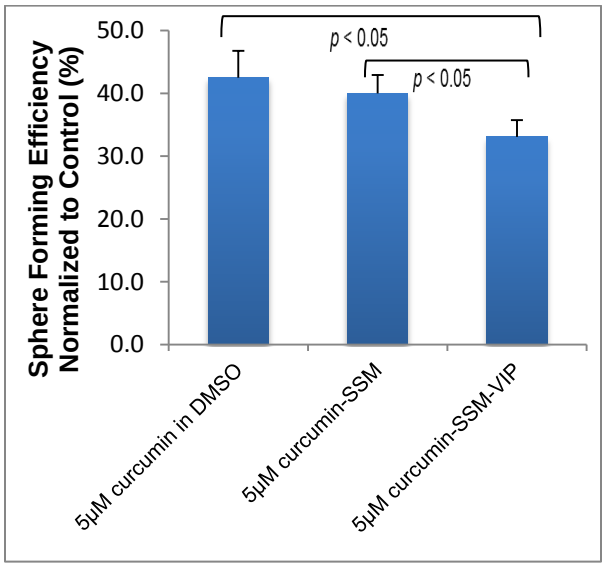

Fig. 8 inhibitory effect of different formulations on tumorsphere formation of MCF-7 cells. MCF-7 cells were treated in sphere-forming conditions and cultured for 7 days. VIP-grafted curcumin nanomicelles significantly increased the inhibitory effect of C-SSM nanomedicine with low curcumin concentration. Data are normalized to relevant controls and presented as mean ± SD of n=3